Comparison of dislocation patterns in cyclically deformed fcc metals

P. Li, Z.F. Zhang,* S.X. Li and Z.G. Wang

Shenyang National Laboratory for Materials Science, Institute of Metal Research, Chinese Academy of Sciences, 72 Wenhua Road, 110016 Shenyang, PR China

Cyclic deformation behaviors of face-centered cubic (fcc) metals, especially Cu and Ag single crystals, were compared. It was found that the dislocation patterns of fatigued Cu and Ag single crystals display similar features with ladder-like persistent slip bands (PSBs). The current finding confirms that, after Cu and Ni, Ag is the third pure fcc metal to form the ladder-like PSB structure. Based on the two-phase model of the saturation shear stress, a new criterion for PSB formation has been established.
© 2008 Acta Materialia Inc. Published by Elsevier Ltd. All rights reserved.

Keywords: Cu and Ag single crystals; Cyclic deformation; Persistent slip bands (PSBs); Dislocations; Two-phase model

In the late 1970s, Mughrabi [1] presented the well-known cyclic stress–strain curve (CSSC) of Cu single crystal with single-slip orientation. The most important and interesting finding in the CSSC is that there exists a plateau region B corresponding to the appearance of persistent slip bands (PSBs). In region B, the plastic strain is mainly localized in the narrow PSBs, and a two-phase (PSBs and matrix) model was proposed to explain the distribution of plastic strain amplitude within PSBs and matrix in fatigued Cu single crystals [2,3]. In order to further reveal the evolution of PSBs, based on the diamond model of Taylor–Nabarro matrix, Neumann [4,5] explored the decomposition of vein structure and the formation of wall structure. It can be regarded as a significant attempt on formation mechanism of PSBs.

Although there has been much literature about dislocation patterns in fatigued Cu single crystals, the real reason for the formation of PSBs is not clear yet. Besides Cu crystals, there are some investigations on the fatigue behaviors of other fcc metals or alloys, such as Ni, Al and Cu–Al alloy single crystals. It seems that the cyclic deformation behaviors and saturation dislocation structures of Ni single crystals are closer to those of Cu single crystals [6–8]. However, the cyclic deformation and dislocation structures of Al and Cu–Al single crystals displayed significantly different features from those of Cu

and Ni single crystals [9–11]. This indicates that different fcc crystals or alloys should behave in quite different fatigue properties and damage mechanisms. Ag is one of the important fcc metals; however, there is virtually no report on the fatigue behavior of Ag crystals, especially dislocation arrangements. In the current research, for the first time, we explore the fatigue dislocation patterns of Ag single crystals in comparison with Cu single crystals to establish their similarities on fatigue damage mechanisms of fcc metals.

It is well known that one important feature of cyclically deformed fcc crystals is the appearance of slip bands (SBs) and deformation bands (DBs). Li et al. [12] have systematically summed up the reason for the formation of various DBs and their relation with SBs. Basically, DBs can be broadly divided into DBI and DBII accordingly to parallel to or perpendicular to SBs. Figure 1a & c and b & d shows the surface deformation morphologies of [$\bar{2}$36] Cu single crystal and [$\bar{2}$39] Ag single crystal used in this experiment, respectively. It can be seen that there is only DBII but no DBI in Cu single crystal. For Ag single crystal, only DBI was formed, but there is no DBII. At high magnification, it can be seen that the plastic strain is mainly localized within the primary SBs, as shown in Figure 1c & d, displaying a typical persistent feature in both Cu and Ag single crystals.

Apart from the surface slip morphology, dislocation configuration with ladder-like PSBs is another important feature after cyclic deformation of fcc crystals. It

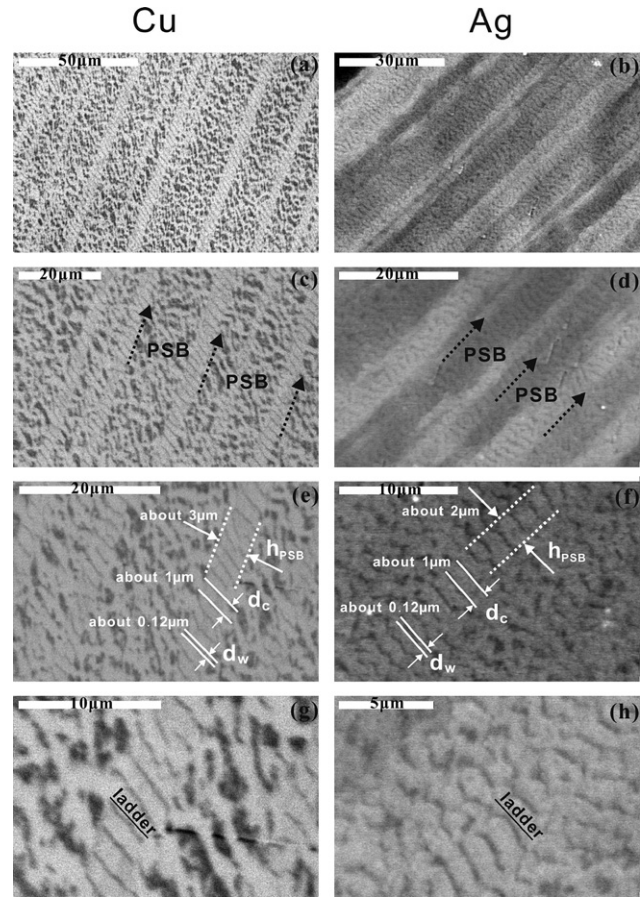* Corresponding author. Tel.: +86 24 23971043; e-mail: zhfzhang@imr.ac.cn
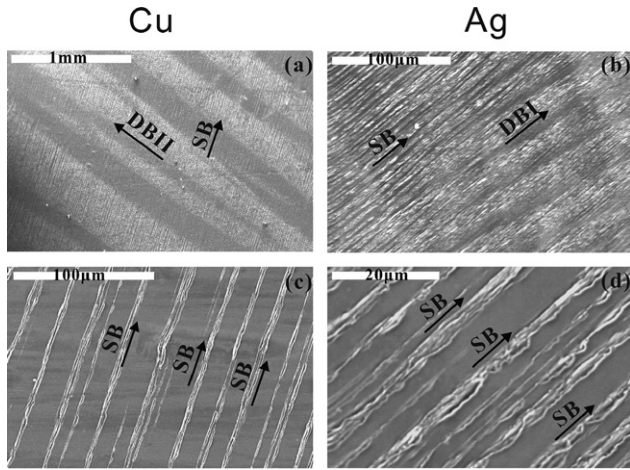
Figure 1. Surface slip morphologies of the fatigued [$\bar{2}36$] Cu and [$\bar{2}39$] Ag single crystals. (a) and (c) Cu single crystal; (b) and (d) Ag single crystal.

Figure 2. Dislocation structures in [$\bar{2}36$] Cu and [$\bar{2}39$] Ag single crystals after cyclic saturation at the plastic shear strain amplitudes of 2.1×10^{-3}. (a), (c), (e) and (g) Cu single crystal; (b), (d), (f) and (h) Ag single crystal.

is well known that when Cu single crystal with single-slip orientation is cyclically deformed in the plastic resolved shear strain amplitude range of $\gamma_{pl} = 6.0 \times 10^{-5}$–$7.5 \times 10^{-3}$, the saturation resolved shear stress is in the range of 28–30 MPa [1,13], and in particular, typical PSBs with ladder-like structure are often formed [2,3]. Since the plastic shear strain amplitudes of Cu and Ag crystals currently selected are just in this range (see Fig. 2), the objective of the present work is to know, besides Cu crystal, whether the regularly arranged dislocation configuration appears or not in Ag single crystal cyclically deformed at the appropriate shear strain amplitude.

Figure 2 shows the dislocation configurations at different magnifications in fatigued [$\bar{2}36$] Cu and [$\bar{2}39$] Ag single crystals. From the observations above, it is apparent that the typical ladder-like PSBs appear in both Cu and Ag single crystals, which correspond well with the surface SBs (see Fig. 1c & d and Fig. 2c & d). Table 1 summarizes some basic data about shear modulus G, stacking fault energy γ_{sf} and Burgers vector b for Al, Cu, Ni, Ag and Cu–Al alloys. It can be seen that obvious PSB-ladder structure can appear only when the ratio of G/γ_{sf} is between 1 and 2. When the ratio G/γ_{sf} is too large or too small, such as in Al and Cu–Al alloys, there will be no PSB-ladder formation [9–11], indicating that the G/γ_{sf} ratio could be employed as the criterion for judging the PSB-ladder formation as discussed below. In addition, we notice that the case of silicon, which possesses the same slip systems as fcc metals but with a friction force, remains to be further analyzed. This material has a ratio of 1.15 and does not form ladder-like structures [14].

For a given shear strain amplitude γ_{pl}, when the cyclic saturation occurs, the volume fractions f_M and f_{PSB} of matrix and PSBs are all constant. The plastic strain amplitudes carried by PSBs and matrix are γ_{PSB} and γ_M, respectively; therefore the average shear plastic strain amplitude can be expressed as [3]:

$$\gamma_{pl} = \gamma_{PSB} f_{PSB} + \gamma_M f_M \tag{1}$$

Table 1. Relationship among stacking fault energy (SFE) γ_{sf}, shear modulus G and PSB formation of different fcc metals at 300 K

| Metal	SFE γ_{sf} (mJ/m^2)	G (Gpa)	Burgers vector b (Å)	PSB-ladder formation	G/γ_{sf} (10^{12} m^{-1})
Al	166–200	25–28	2.86	No	1/6–1/8
Ni	80–128	75–80	2.49	Yes	1–2
Cu	40–78	40–75	2.55	Yes	1–2
Ag	16–22	19–44	2.50	Yes	1–2
Cu-10 at% Al	10	35–41	—	No	3.5–4
Cu-16 at% Al	6	35–41	—	No	6–7
Reference	[15–18]	[19]	[18]	[15] and present result	

(Note: so far, no typical PSB-ladder is seen in Al crystals, though the result from Ref. [15] is yes.)

Figure 3a illustrates the classical two-phase model on macroscopic scale. But this model cannot explain why the PSBs are formed and how the dislocation configurations evolve; therefore, it is necessary to analyze the structures of PSBs on mesoscopic, even on microscopic scales. As shown in Figure 3b, the composite model of PSB structure can be further classified into dipole walls and channels on mesoscopic scale. The dipole walls have high dislocation densities ρ_w and the channels contain low dislocation densities ρ_c. The mean wall thickness d_w, together with the mean channel width d_c and the
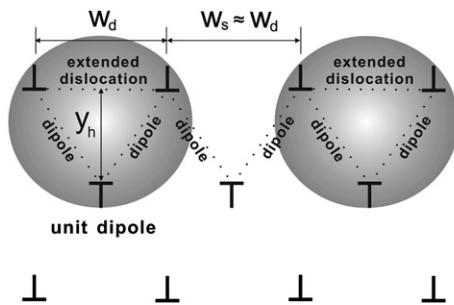
(a) macroscopic scale
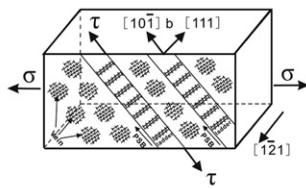
(b) mesoscopic scale
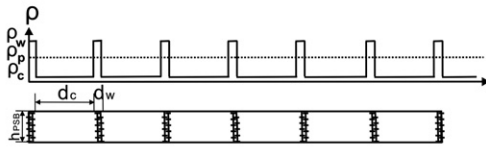
(c) microscopic scale

Figure 3. Schematic diagram of the typical saturation dislocation patterns in cyclically deformed fcc crystals on (a) a macroscopic, (b) a mesoscopic and (c) a microscopic scale.

mean height h_{PSB}, constitutes the geometrical parameter of individual PSB.

It is well known that dislocation movement in fcc metals is dominated by the dissociated dislocation. Figure 3c describes the dislocation array in the dipole walls on a microscopic scale. Each extended dislocation is composed of two dissociated partial dislocations. Assuming that the extended dislocations in the dipole wall possess the regular and tight array, the space w_s between the dissociated dislocations under such array can be estimated by the dislocation density (10^{15-16} m^{-2} [20]) of the dipole wall. The results showed that the space (~5 nm) and the width (3–5 nm [18]) of the extended dislocations can be regarded as approximately equal; accordingly, each stable structure is composed of two pairs of dipoles with positive–negative edge partial dislocations and an extended dislocations. Therefore it is suggested that such stable structure named by unit dipole approximates to an equilateral triangle, which will be elaborated in the following calculation.

Since the PSB can be regarded as a composite consisting of soft channels and hard walls [21], the plateau stress τ_s should be a function of the flow stresses of the channels τ_c and the walls τ_w in terms of mixture rule [21,22]:

$$\tau_s = f_w \tau_w + (1 - f_w)\tau_c \qquad (2)$$

Here, f_w is the area fraction of the walls. The local stress τ_c of the channels is assumed to be equal to the stress necessary to bow-out screw dislocations. For screw dis-

location segments extended through the whole channel, the line tension approximation leads to [7]:

$$\tau_c = \alpha Gb/d_c + \tau_c^F \qquad (3)$$

where α is a geometrical factor, G denotes the shear modulus, τ_c^F is the friction stress component which results from the interaction of the screw dislocations with glide obstacles.

For calculating the local flow stress in walls, we follow the approach of Essmann and Differt [8], who considered a test dislocation of edge type moving through an arrangement of dipoles. They found that τ_w is proportional to the mean dipole height y_h and to the dipole density ρ_d. If adding the term of friction stress, we get

$$\tau_w = D^* y_h \rho_d + \tau_w^F \qquad (4)$$

where $D^* = 1.25\, Gb/[\pi(1-v)]$ and v denotes the Poisson's ratio ($v = 0.32$).

Referring to Eqs. (3) and (4), the flow stresses τ_c and τ_w can be given and further taking them into Eq. (1), the saturation shear stress τ_s will be obtained. However, firstly we need to estimate the values of the friction stresses τ_c^F and τ_w^F. According to the analysis from Bretschneider et al. [7], there are two additive friction stresses $\tau_c^F \approx 0.25\tau_c$ and $\tau_w^F \approx 0.25\tau_w$, respectively. Assuming $\alpha = 2.0$ [7], Eq. (3) can be simplified as:

$$\tau_c = \frac{8Gb}{3d_c} \qquad (5)$$

Secondly, because of the lack of experimental data for the microscopic parameters y_h and ρ_d, Eq. (4) cannot be used well. But a scaling relation $\rho_d y_h^2 \approx 1/30$ was introduced by Tippelt et al. [23]. In comparison with Figure 3c, we can adjust the relation into $\rho_d y_h w_d = n$, where w_d denotes the width of extended dislocation, and assuming that the stable structure of dipoles meets the relation of $w_d/y_h \approx 1.5$[20], eventually the relation can be obtained

$$\rho_d y_h \approx 1/20w_d \qquad (6)$$

Substituting Eq. (6), $D^* = 1.25Gb/[\pi(1-v)]$ and $w_d = (2-v)Gb^2/[(1-v)8\pi\gamma_{sf}]$ into Eq. (4), the flow stress τ_w can be simplified as follows:

$$\tau_w = \frac{2\gamma_{sf}}{3(2-v)b} \qquad (7)$$

Ultimately, based on Eqs. (5) & (7), Eq. (2) can be rewritten as:

$$\tau_s = f_w \frac{2\gamma_{sf}}{3(2-v)b} + (1 - f_w)\frac{8Gb}{3d_c} \qquad (8)$$

Before further estimating the saturation shear stress, the geometric structure parameters of PSBs must be known. Figure 2e & f indicates several structure parameters of the PSBs in Cu and Ag single crystals: i.e. channel width d_c of 1 ± 0.2 μm; wall thickness d_w of 0.12 μm and PSB height h_{PSB} of about 2–3 μm. The above data are consistent with the results from the previous reports [20]. This clearly demonstrates that the formation of PSBs is necessary to match the geometric parameters because the PSBs in Ag and Cu single crystals possess a similar geometric structure. The similar structure parameters also appear in fatigued Ni single crystal [24]. Together with the saturation stress τ_s and the

Table 2. The saturation stress value and geometrical parameters of PSBs in different fcc metals

Metal	τ_s^E (MPa)	d_c	d_w	h_{PSB}	$f_w = d_w/(d_c + d_w)$	τ_s^T (MPa)	Reference
Ni	50	1.2	0.15 ± 0.02	~4	~10%	~51	[24]
Cu	26	1 ± 0.2	0.12 ± 0.02	~3		~29	Present result
Ag	18	1 ± 0.2	0.12 ± 0.02	~2		~20	Present result

(Note: τ_s^E and τ_s^T denotes the experimental value and the theoretical value of the saturation shear stress, respectively.)

volume fraction f_{PSB} of the PSBs, these geometric parameters of the wall-channel structure in the PSBs can be summarized in Table 2.

If considering the constants γ_{sf}, G and b in Table 1 and the experimental values d_c and f_w in Table 2, one can estimate the saturation shear stress τ_s^T for Ni, Cu and Ag, which are in good agreement with the experimental values τ_s^E. Taking Ni as an example, the estimated flow stresses τ_c and τ_w are very reasonable, namely $\tau_c \approx 41.7$ MPa and $\tau_w \approx 127$ MPa, respectively. Finally in terms of Eq. (2), the plateau saturation resolved shear stress is estimated $\tau_s^T \approx 51$ MPa, which is very close to the experimental data. For Cu and Ag crystals, the theoretical values are listed in Table 2 and also correspond to their experimental results.

Furthermore, if both sides of Eq. (8) are divided by G, it can be simplified as

$$\tau_s/G = \frac{M}{G/\gamma_{sf}} + \frac{N}{d_c} \tag{9}$$

where there are two constants $M = \frac{2f_w}{3(2-\nu)b}$ and $N = \frac{8(1-f_w)b}{3}$. Thus the whole equation consists of the three components of τ_s/G, G/γ_{sf} and d_c. Here, τ_s/G denotes the difficulty degree of slip; G/γ_{sf} indicates the ability of the stacking fault aggregation; d_c denotes the geometrical structure of PSBs. At room temperature, for different fcc metals, d_c is almost unchanged, so the equation is mainly determined by the first two terms. When the ability of slip is strong enough, the dislocations that have been gathered together are unstable, and will be further broken up and therefore cannot form a stable dislocation configuration, such as Al. When the ability of slip is too weak, the dislocations cannot complete the aggregation and likewise will not form the dislocation configuration, such as Cu–Al. Only when the abilities of slip and aggregation are both appropriate, the classical PSB-ladder structure is able to appear, such as Ni, Cu and Ag with $G/\gamma_{sf} = 1$–2.

In summary, except for Cu single crystal, the ladder-like PSBs can also be found in Ag single crystal after the cyclic saturation. Li et al. [25] has described the dislocation configurations in Cu single crystals with various orientations; Holste et al. [6,26,27] systematically summarized the CSSC and dislocation configuration of single-slip oriented Ni single crystals at different temperatures. The current study confirms that, after Cu and Ni, Ag is the third fcc pure metal, which can form the ladder-like PSB structure. Based on the flow stresses τ_c, τ_w and the two-phase model of the saturation shear stress τ_s, a new criterion is proposed for judging whether the PSB-ladder structure can form in a given fcc metal. This will be conducive to estimate the cyclic deformation behaviors of different fcc metals.

[1] H. Mughrabi, Mater. Sci. Eng. 33 (1978) 207.
[2] J.M. Finney, C. Laird, Philos. Mag. 31 (1975) 339.
[3] A.T. Winter, Philos. Mag. 30 (1974) 719.
[4] P. Neumann, Mater. Sci. Eng. 81 (1986) 465.
[5] P. Neumann, in: R.W. Cahn, P. Hassen (Eds.), Physical Metallurgy, Elsevier, Amsterdam, 1983, p. 1554.
[6] C. Holste, Philos. Mag. 84 (2004) 299.
[7] J. Bretschneider, C. Holste, B. Tippelt, Acta Mater. 45 (1997) 3775.
[8] U. Essmann, K. Differt, Mater. Sci. Eng. 208 (1996) 56.
[9] O. Vorren, N. Ryum, Acta Metall. 35 (1987) 855.
[10] H. Inui, S.I. Hong, C. Laird, Acta Metall. 38 (1990) 2261.
[11] X.M. Wu, Z.G. Wang, G.Y. Li, Mater. Sci. Eng. 314 (2001) 39.
[12] S.X. Li, X.W. Li, Z.F. Zhang, Z.G. Wang, K. Lu, Philos. Mag. 82 (2002) 3129.
[13] A.S. Cheng, C. Laird, Mater. Sci. Eng. 51 (1981) 55.
[14] M. Legros, A. Jacques, A. George, Philos. Mag. 82 (2002) 3275.
[15] Z.R. Wang, Philos. Mag. 84 (2004) 351.
[16] M. Rester, C. Motz, R. Pippan, Scripta Mater. 58 (2008) 187.
[17] L.E. Murr, Interfacial Phenomena in Metals and Alloys, Addison Wesley, Reading MA, 1975, p. 145–48.
[18] D.Z. Yang, Dislocation and Metal Strengthening Mechanism, Harbin Institute of Technology Press, Harbin, 1991, p. 71.
[19] Z.S. Hou, G.X. Lu, Principles of Metallography, Shanghai Science and Technology Press, Shanghai, 1990, p. 174.
[20] S. Suresh, Fatigue of Materials, 2nd ed., Cambridge University Press, Cambridge, 1998, p. 38, 41.
[21] H. Mughrabi, in: O. Brulin, R.K.T. Hsieh (Eds.), Proceedings of the Fourth International Conference on Continuum Models of Discrete systems, Continuum Models of Discrete systems, 1981, p. 241.
[22] H. Mughrabi, Acta Metall. 31 (1983) 1367.
[23] B. Tippelt, J. Bretschneider, P. Hähner, Phys. Status Solidi A 163 (1997) 11.
[24] A. Schwab, J. Bretschneider, C. Buque, C. Blochwitz, C. Holste, Philos. Mag. Lett. 74 (1996) 449.
[25] X.W. Li, Z.F. Zhang, Z.G. Wang, S.X. Li, Y. Umakoshi, Defects Diffusion forum 188–190 (2001) 153.
[26] C. Holste, J. Bretschneider, B. Tippelt, Mater. Sci. Eng. 234–236 (1997) 743.
[27] P. Hähner, B. Tippelt, C. Holste, Acta Mater. 46 (1998) 5073.